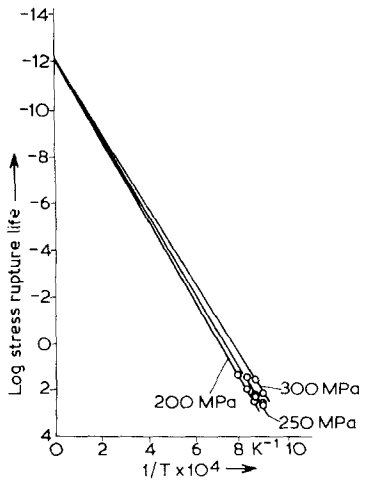

Figure 5 Log time–inverse temperature plot.

with

$$bC = c \quad \text{and} \quad T \log t = z$$

and one obtains

$$\log t_B = \log a + cT + bz.$$

The constant $\log a$, is found from the regression analysis as well as the partial coefficients c and b, where the Larson–Miller constant C is given by

$$C = \frac{c}{b}.$$

Using the values given in Table I, a C value of 12.3 was obtained using a Wang 2200 Series Program which correlates extremely well with the graphical result.

The constant C can also be determined using a technique proposed by Larson and Miller [8], namely a log time–inverse temperature plot. This method has been used by Buchanan and Tarshis [9]. Fig. 5 shows such a plot which, due to the lack of data, can only poorly indicate that C lies between 12 and 13. An alternative method proposed by Woodford [10] of solving simultaneous equations to give a constant parameter value at stresses where results at two or more test temperatures are available, gives variable values for C.

In summary, this study shows that the C constant has to be adjusted to the material in question and that in this case a modification of $C \sim 12$ reasonably correlates the data.

Acknowledgement

Part of this work was supported by the German Ministry of Research and Technology (BMFT).

References

1. E.R. THOMPSON and F.D. LEMKEY, *Met. Trans.* **1** (1970) 2799.
2. E.R. THOMPSON, D.A. KOSS and J.C. CHESNUTT, *ibid* **1** (1970) 2807.
3. A.R. NICOLL and P.R. SAHM, Proceedings of the International Conference on Composite Materials, Vol. 1 (1975) pp. 904–917.
4. K. FRITSCHER and G. WIRTH, *ibid*, Vol. 2 pp. 597–603.
5. R.F. VANDERMONSEN *et al.*, *Cobalt* **2** (1973) 33.
6. P.R. SAHM, *High Temp. High Press.* **7** (1975) 241.
7. D.A. WOODFORD, *Mat. Sci. Eng.* **15** (1974) 169.
8. F.R. LARSON and J. MILLER, *Trans. AIME* **6** (1975) 766.
9. E.R. BUCHANAN and L.A. TARSHIS, *Met. Trans.* **5** (1974) 1413.
10. D.A. WOODFORD, *ibid* **8A** (1977) 639.
11. P.R. SAHM and U.W. HILDEBRANDT, BMFT-NTS 37 Final Report (1978).
12. G. ZWINGMAN and K.F. ZIMMERMAN, *Metall.* **31** (1977) 746.

Received 18 October
and accepted 20 November 1978

A. R. NICOLL
Brown Boveri & Cie AG
Research Centre,
Heidelberg, West Germany

Hot-pressing diagrams for f c c metals

Ashby [1] has constructed sintering diagrams (log (a/R) versus T/T_m) which identify, at a given particle size R, neck size a, and reduced temperature T/T_m, the dominant mechanism. As various mechanisms contribute simultaneously to the neck growth, and as the different rates are functions of a/R, the boundaries of these fields are obtained by equating pairs of rate equations and solving for neck size as a function of temperature. The aim of this communication is to extend such diagrams to hot-pressing.

Let us first return to sintering diagrams. The

0022–2461/79/071761–05 $2.50/0

generally accepted equations for neck growth of two spheres are the following.

For *surface diffusion from surface sources*, the neck radius a, at time t is given [2, 3] by

$$\frac{a^7}{R^3} = \frac{56\gamma\Omega}{kT}\delta_s D_s t, \tag{1}$$

where δ_s is the thickness of the high diffusivity surface layer (about one interatomic spacing), D_s the surface self-diffusion coefficient, γ the surface energy, and Ω the atomic volume.

For *grain-boundary diffusion from the grain-boundary sources* [4, 5] one has

$$\frac{a^6}{R^2} = \frac{96\gamma\Omega}{kT}\delta_B D_B t, \tag{2}$$

where δ_B is the grain-boundary thickness, and D_B the grain-boundary diffusion coefficient.

For *lattice diffusion from surface sources* [2] one has

$$\frac{a^5}{R^2} = \frac{40\gamma\Omega}{kT} D_L t, \tag{3}$$

and for lattice diffusion from the grain-boundary sources [6, 7]

$$\frac{a^5}{R^2} = \frac{80\gamma\Omega}{kT} D_L t \tag{4}$$

where D_L is the lattice diffusion coefficient.

Owing to the uncertainty on the exact value of the fillet radius r, the numerical constants in Equations 1 to 4 must be taken as approximate. For surface diffusion, for example, Rockland [3] proposes 34 instead of 56, Wilson and Shewmon [6] and Ashby [1] propose 112, and Nichols and Mullins [8] obtain 28. Moreover, for lattice diffusion from grain-boundary an alternative solution corresponding to another diffusion length was proposed by Coble [4]:

$$\frac{a^4}{R} = \frac{32\gamma\Omega}{kT} D_L t.$$

We will follow Ashby [1] in the choice of Equation 4.

Ashby [1] used elaborate curvature difference for diffusion, but for stage 1 and 2 sintering, the following approximation appears to be sufficient. By merely using the derivatives of Equations 1, 2 and 4, the rate ratios are

$$\frac{\dot{a}_L}{\dot{a}_B} = \frac{3RD_L}{2\delta_B D_B}\left(\frac{a}{R}\right) \tag{5}$$

$$\frac{\dot{a}_B}{\dot{a}_s} = \frac{2\delta_B D_B}{\delta_s D_s}\left(\frac{a}{R}\right) \tag{6}$$

$$\frac{\dot{a}_L}{\dot{a}_s} = \frac{3RD_L}{\delta_s D_s}\left(\frac{a}{R}\right)^2. \tag{7}$$

As diffusion coefficients are thermally activated, it is more convenient to use Arrhenius plots (log (a/R) versus T_m/T) for the boundaries separation the various field will be straight lines. Furthermore, as activation energies are function of the melting point alone, it is possible to give master curves valid for any fcc metal. Some generally accepted values for pre-exponential factors and activation energies for fcc metals are the following:

for volume diffusion

$$D_{Lo} = 0.5\ \text{cm}^2\ \text{sec}^{-1}$$
$$Q_L = 17.5\,RT_m;$$

for surface diffusion [9]

$$\left.\begin{aligned} D_{so} &= 740\ \text{cm}^2\ \text{sec}^{-1} \\ Q_s &= 15\,RT_m \end{aligned}\right\} \quad T > 0.75\,T_m$$

$$\left.\begin{aligned} D_{so} &= 1.4\ 10^{-2}\ \text{cm}^2\ \text{sec}^{-1} \\ Q_s &= 6.5\,RT_m \end{aligned}\right\} \quad T < 0.75\,T_m;$$

for boundary diffusion, D_B depends on structure and orientation of the boundary, being related to the grain-boundary energy by the Borisov formula [10, 11], but the following mean value can be used [12]

$$D_{Bo} = 0.3\ \text{cm}^2\ \text{sec}^{-1}$$
$$Q_B = 9\,RT_m.$$

Fig. 1 is such a map constructed for four radii, with $\delta_s = 3 \times 10^{-8}$ cm and $\delta_B = 5 \times 10^{-8}$ cm. One can see that surface diffusion is dominant at low temperature and that grain-boundary diffusion disappears when the radius R increases. The different picture given by Ashby for copper and silver arises from the high values of Q_s he used: respectively $18\,RT_m$ and $25.5\,RT_m$ whatever the tem-

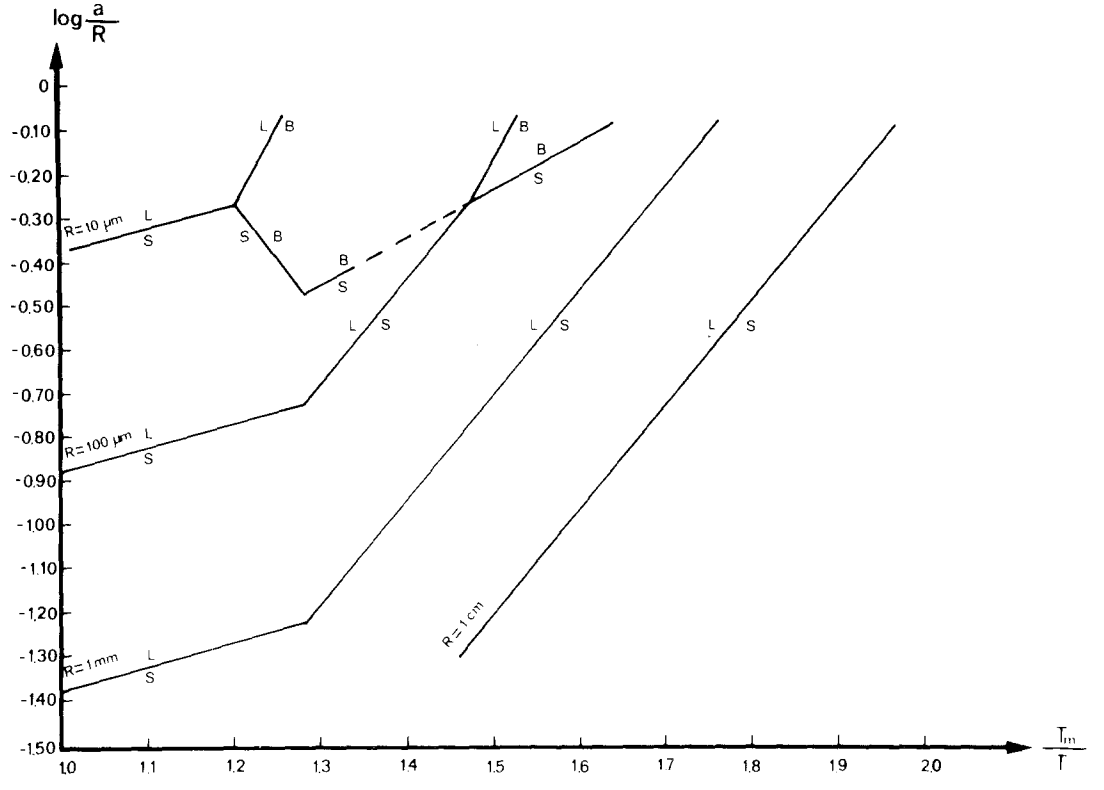

Figure 1 Sintering diagram for f c c spheres.

perature. As seen from Equation 6 the boundary between surface diffusion and grain-boundary diffusion is independent of the radius R, so that the triple point (in fact, a small triangle) moves along the curve when R varies. The field corresponding to dominant grain boundary disappears for $R > 400\,\mu m$ or $T < 0.6\,T_m$; that corresponding to surface diffusion decreases in favour of volume diffusion when R increases. This influence of the radius is in conformity with Herring's scaling law [13]: if $R_2 = \lambda R_1$, the time required to produce geometrically similar configurational changes is given by $\Delta t_2 = \lambda^4 \Delta t_1$ for surface diffusion, and by $\Delta t_2 = \lambda^3 \Delta t_1$ for volume diffusion. So, at a given temperature and a/R, the volume diffusion becomes predominant as R increases. Notice that the a/R values corresponding to elastic adhesion depend on the nature of R metal and do not appear on the figure. Large values of radius R correspond to the fact that the author has in mind adhesion of rough solids at high temperature.

As in Herring–Nabarro and Coble creep, the applied pressure increases the vacancy deficit at the grain boundary and enhances the mass transfer from the grain boundary to the neck (by boundary diffusion, or lattice diffusion). When a force P is applied to two spheres, the applied pressure at the grain boundary is $\sigma = P/(\pi a^2)$, and the pressure difference between the grain boundary and the neck subsurface increases from γ/r to $\gamma/r + \sigma$. So, as suggested by Coble [14], γ in Equations 2 and 4 must be expanded into $\gamma + \sigma r = \gamma + P/(4\pi R)$. This corrective term may be important in hot-pressing; assuming the particle packing to be simple cubic, the relation between the force P and the mean pressure P_a applied to the powder is $P = 4R^2 P_a$; hence the term $\gamma' = P/(4\pi R) = P_a R/\pi$ [14] may be as high as $10^3\gamma$. Equations 5, 6 and 7 become:

$$\frac{\dot{a}_L}{\dot{a}_B} = \frac{3RD_L}{2\delta_B D_B}\left(\frac{a}{R}\right)\frac{K_L}{K_B} \tag{8}$$

$$\frac{\dot{a}_B}{\dot{a}_s} = \frac{2\delta_B D_B}{\delta_s D_s}\left(\frac{a}{R}\right)K_B \tag{9}$$

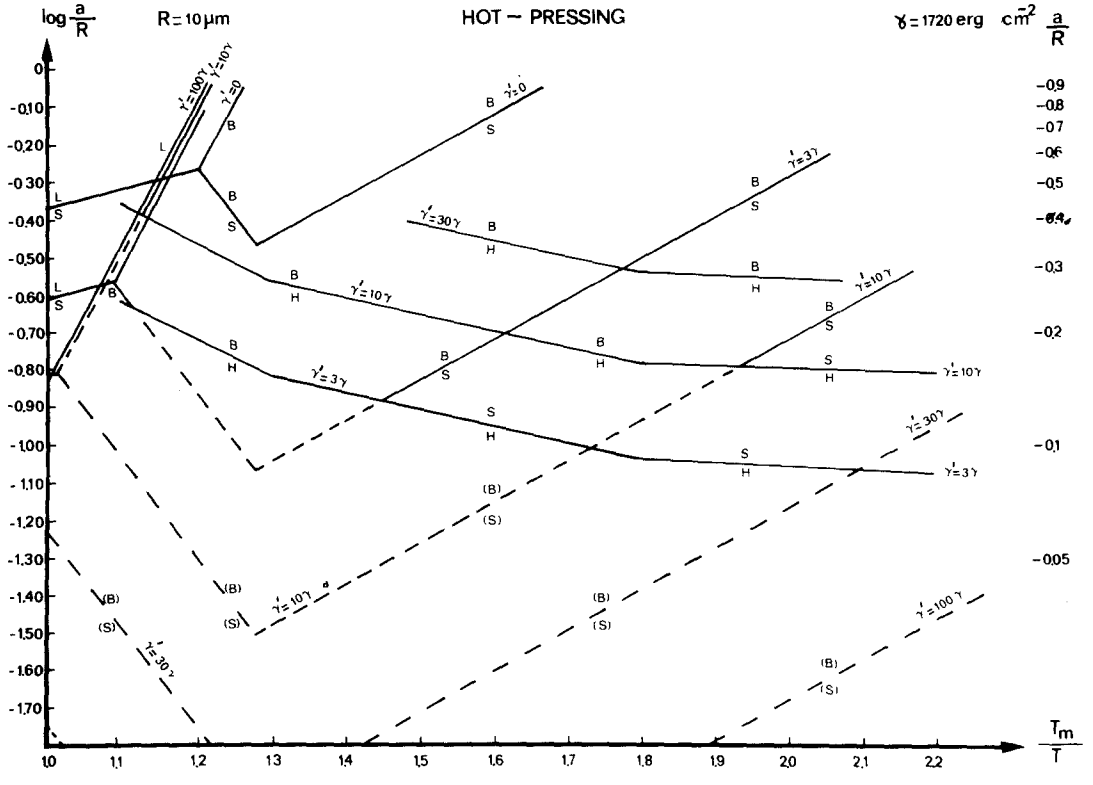

Figure 2 Hot pressing diagram for f c c spheres (radius 10 μm). The hot hardness limits are for copper ($\gamma = 1720\,\mathrm{mJ\,m^{-2}}$).

$$\frac{\dot{a}_L}{\dot{a}_s} = \frac{3RD_L}{\delta_s D_s}\left(\frac{a}{R}\right)^2 K_L \qquad (10)$$

with

$$K_B = 1 + \frac{\gamma'}{\gamma}$$

$$K_L = 1 + \frac{2\gamma'}{3\gamma}.$$

Figs. 2 and 3 show that hot-pressing dramatically increases the field (B) corresponding to grain-boundary diffusion. However, the pressure at the boundary cannot exceed the hardness value H. So, for higher stresses, stage 1 does not differ from a mutual hot hardness, hence, hot-pressing is by power law creep. We could tentatively use hot-hardness equations [16, 17] to describe the increase of neck radius with time, but the problem of the activation energies for hot hardness is still open. For a very rough estimate of the positions of the creep field (H) in the hot-pressing diagram, it is more direct to use hardness experimental values, as given by Lozinskii [18] (Vickers diamond, load 10 N, contact time 1 min). So, a very approximative value of a/R first reached by plastic flow is

$$\frac{a}{R} = \left(\frac{P}{\pi R^2 H}\right)^{\frac{1}{2}} = \left(\frac{4P_a}{\pi H}\right)^{\frac{1}{2}} = \left(\frac{4\gamma'}{HR}\right)^{\frac{1}{2}}. \qquad (11)$$

The case of copper is described in Figs. 2 and 3. The value $\gamma = 1720\,\mathrm{mJ\,m^{-2}}$ was used, as in Ashby's [1] paper. As γ' increases, the field corresponding to plastic flow (H) increases and the field (S) corresponding to surface diffusion may disappear. Notice that γ' is proportional to R for a given pressure P_a, so that the "hardness curves" of Fig. 2 that can be superimposed on those of Fig. 3 correspond to the same pressure P_a on a powder. (The represented pressures, 0.16 to $16\,\mathrm{MNm^{-2}}$, are

*Even the action of molecular forces under zero load is not negligible. Using the apparent Hertz load $P_1 = 6\pi wR$ [15], where w is the work of adhesion, one has $\gamma' = 3w/2$. Taking the approximation $w = 2\gamma - \gamma_B = \frac{5}{3}\gamma$, where γ_B is the grain-boundary energy, $\gamma' = 2.5\gamma$. But for small radii, one can think that this stress is first relaxed by plastic flow and does not act in subsequent diffusion processes.

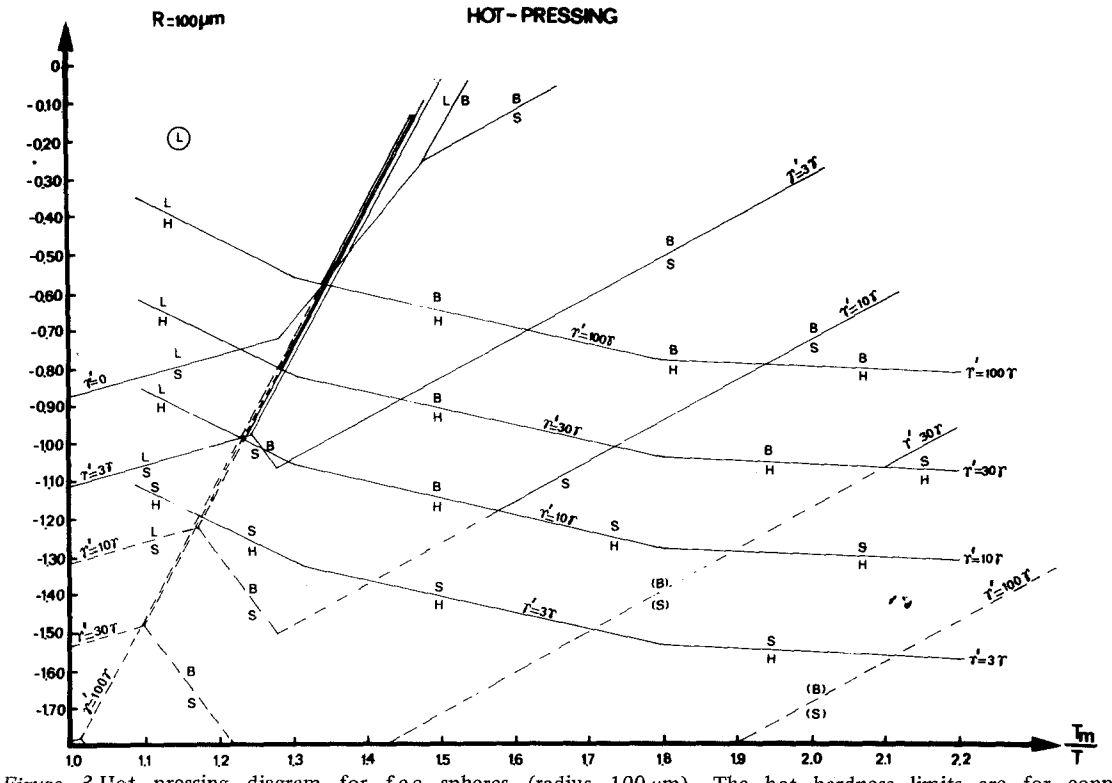

Figure 3 Hot pressing diagram for fcc spheres (radius 100 μm). The hot hardness limits are for copper ($\gamma = 1720\,\mathrm{mJ\,m^{-2}}$).

moderate pressures for hot-pressing.) Recall moreover that the boundary B – S is independent of the radius.

The construction of such diagrams is useful to understand the mechanisms of hot-pressing or adhesion of rough surfaces at high temperature.

Acknowledgement

Support of this research by the D.G.R.S.T. (no. 78.7.0273) is gratefully acknowledged.

References

1. M. F. ASHBY, *Acta Met.* **22** (1974) 275.
2. G. C. KUCZYNSKI, *Trans. AIME* **185** (1949) 169.
3. J. G. R. ROCKLAND, *Acta Met.* **14** (1966) 1273.
4. R. L. COBLE, *J. Amer. Ceram. Soc.* **41** (1958) 55.
5. D. L. JOHNSON, *J. Appl. Phys.* **40** (1969) 192.
6. T. L. WILSON and P. G. SHEWMON, *Trans. AIME* **236** (1966) 48.
7. W. D. KINGERY and M. BERG, *J. Appl. Phys.* **26** (1955) 1205.
8. F. A. NICHOLS and W. W. MULLINS, *ibid* **36** (1965) 1826.
9. N. A. GJOSTEIN, in "Surfaces and Interfaces", Vol. 1, edited by J.J. Burke, N.L. Read and V. Weiss. (Syracuse, 1967) pp. 271–304.
10. P. GUIRALDENQ, *J. Phys.* **36** (1975) C4-201.
11. D. GUPTA, *Met. Trans.* **8A** (1977) 1431.
12. N. A. GJOSTEIN, A.S.M Seminar Diffusion (1973) p. 271.
13. C. HERRING, *J. Appl. Phys.* **21** (1950) 301.
14. R. L. COBLE, *ibid* **41** (1970) 4798.
15. K. L. JOHNSON, K. KENDALL and A. D ROBERTS, *Proc. Roy. Soc. A* **324** (1971) 301.
16. T. O. MULHEARN and D. TABOR, *J. Inst. Metals* **89** (1960) 7.
17. A. G. ATKINS, A. SILVERIO and D. TABOR, *J. Inst. Metals* **94** (1966) 359.
18. M. G. LOZINSKII, "High temperature Metallography", (Pergamon, Oxford, London, New York, Paris, 1961).

Received 31 October
and accepted 27 November 1978.

D. MAUGIS
Equipe de Recherche de Mécanique des Surfaces,
C.N.R.S., 1 place A. Briand,
92190 Meudon,
France